Keywords: *Zinc Containment, TEF, Contamination Control*

Retention: *25 yrs-**10561***

SRNL-STI-2012-00616

Effectiveness of Copper and Bronze for Zinc Capture

P.S. Korinko

Oct. 15, 2012

This Page Intentionally Left Blank

SRNL-STI-2012-00616

Effectiveness of Copper and Bronze for Zinc Capture

Table of Contents

List of Tables

List of Figures

SRNL-STI-2012-00616

Effectiveness of Copper and Bronze for Zinc Capture

Summary

A series of experiments was conducted to determine the efficacy of using copper and bronze sheet and screen under high vacuum conditions to capture zinc vapor. The experiments were conducted in a parametric manner using a fixed zinc vaporization temperature (350°C) but varying the filter temperature from ambient to 550°C. Consistent with previous work, metallic zinc was deposited at low temperatures, but the deposit was non-adherent. At an intermediate temperature range (350-450°C), the deposit formed an alloy with both copper and bronze materials. At higher temperatures ($\geq$ 500°C) the zinc did not deposit on the surfaces likely due to its high vapor pressure. Additional testing to optimize the zinc "getter" chemistry and surface condition is warranted.

Background

After the TPBARs that were irradiated in the Tennessee Valley Authority's (TVA) Watts Bar Nuclear (WBN) reactor in fuel cycle 6 were extracted in the Tritium Extraction Facility (TEF), a radiation survey was conducted. During the survey, a radiation technician detected a slightly higher radiation signature than the previous baseline. Upon further examination, it was determined that the increase was due to the presence of zinc 65 (^{65}Zn) isotope that had deposited in the outlet of the turbomolecular pump. An investigation was undertaken to determine the source of the deposit and to determine how potentially transportable the ^{65}Zn may be (1). Through a forensic examination of the piping components and deposit, it was determined that the zinc was deposited as a metal rather than an oxide. It was further determined that the zinc was adherent to the pipe sidewalls. To minimize the potential for ^{65}Zn migration, a series of experiments was conducted to establish optimized conditions to capture the ^{65}Zn on a filter placed in the piping of the glovebox (2, 3, 4, 5, & 6) rather than have it migrate to other areas of the facility. A stainless steel coalescing filter with a 20 µm pore diameter heated to 200°C was determined to be the optimal conditions to capture and retain the ^{65}Zn.

Although effective, this solution results in the gamma emitting zinc being trapped and contained in an area of the facility that is designed for beta; while it is not a significant dose issue during the time that TEF is in "responsive operations" where a single extraction is completed each year and there is ample time to schedule and complete the required filter maintenance/replacement, as tritium production increases this opportunity will become more challenging. Consequently, a method that contains the ^{65}Zn behind the shield wall in the furnace module is desirable. In order to implement a suitable "fix" there are a number of considerations that need to be addressed: 1) there is limited space in which to place an active zinc getter in the furnace module, however, there are some possibilities; 2) the fix must react with zinc but not hydrogen, i.e., must not form stable hydrides; and 3) the material must be stable in the TEF process gas and not react in such a manner that it becomes inert to the zinc vapor. These

restrictions on the proposed fix revealed that copper and copper alloys may be capable of meeting the requirements (2, 5).

This report describes the apparatus that was designed and built to vaporize and capture zinc vapor on copper screen and bronze screen and bronze strips at Zn fluxes that are significantly higher than those

Figure 1. Test apparatus showing controllers (left) and mantle and filter heater (right) and filter basket.

observed or expected in the TEF. Testing was conducted at a fixed vaporization temperature of 350°C and at filter temperatures ranging between room and 550°C.

Experimental

An all metal seal (i.e., Conflat Flanges) high vacuum deposition and capture system was designed and fabricated primarily from off-the-shelf components. Photographs of the apparatus and filter holder are shown in Figure 1. This system has a four inch half nipple that is used as a "zinc pot". The zinc pot is connected to a full nipple that contains the zinc filter support. A wide range gauge (KJ Lesker Pirani – hot cathode (WRG)) is placed above the zinc pot and a 10 Torr Baratron is connected to this chamber as well. The system subsequently pumps through a 200°C heated trap that contains steel wool. The trap is heated using heater tape with three thermocouples attached for control, over-temperature and reference. A scroll pump is used to rough pump the system and turbomolecular pump is used to achieve high vacuum ($P<1x10^{-5}$ Torr). A second wide range gauge is present on the turbomolecular pump. A mantle heater is used to heat the zinc pot to 350°C. The Zn pot has three type K thermocouples attached, one for control, one over-temperature and one reference. The filter was initially heated using glass covered heater tape; however, this heat source was inadequate to reach 500°C so a Watlow split cylinder ceramic fiber heater was installed over the heated filter area. It was also insulated with ceramic wool. Four type K thermocouples are installed on the filter hot zone, one control, one over-temperature, and two reference thermocouples, one positioned at the top of the filter and the second positioned at the bottom. The internal temperature of the zinc pot and filter was monitored using an Omega thermocouple reader that reads twelve thermocouples. Ten thermocouple elements were spaced 1.125 inches apart and read on channels 1-10. The filter was positioned between the seventh and eighth elements; seven was at the bottom. Channels 11 and 12 were used to monitor other temperatures on the assembly.

Tests were conducted consistent with written R&D Directions (7). Zinc was weighed and placed in the zinc pot, the screen and any strip materials were also weighed and placed in the filter holder. The compositions of the screen and bronze strips are listed in Table 1. The filter holder was placed into the full nipple on the hang-down filter holder. A new copper gasket was installed on the flange and the bolts were tightened in a cross pattern. The system was evacuated for a minimum of 12 hours after reassembly to ensure that acceptable vacuum levels were achieved. The base vacuum, as measured by the WRG over the turbomolecular pump, was typically in the mid 10^{-7} Torr range. The heaters were programmed so that they automatically heated at the desired rate and held for the target time. The trap was heated at 20°C/min to 200°C and held for 9 hours - 25 minutes, the filter was heated to the desired setpoint in 45 minutes and held for 9 hours, and the zinc pot was heated at 8 to 10°C/min to 350°C after a four hour delay for the filter area to reach its steady state temperature. The temperature and pressure data were recorded at approximately 15 second intervals using a custom Labview data acquisition program. Tests were run at room temperature to 550°C. The elevated temperature tests were run at a filter controller temperature of 250°C to 550°C in 50°C increments to determine if there is an optimal temperature range for deposition and capture.

Table 1. Composition of materials tested.

Designation	Copper	Sn	P
Cu-Screen	100%		
Br-Screen	90.75-95.75	9.0-4.0	0.25
Br-Strips	95.15	4.61	0.17

After the system cooled, the apparatus was brought up to atmospheric pressure by venting with helium. The screen and strip samples were removed and weighed on an Ohaus Discovery analytical scale and photographed using a Panasonic Lumix LZ5 digital camera. Unexposed screen and strip materials were included in the photographic comparisons as needed. Select samples were examined using XRD, SEM, metallography and XRF. XRD was accomplished using a Rigaku Copper K_α at an accelerating voltage of 20 KeV was used. The samples were scanned from $2\theta = 20$ to 130°. Intensity data was collected. The d-spacing and lattice parameters were determined. Recall that peaks occur where the Bragg law is satisfied.

Equation 1 $$n\lambda=2d\sin(\theta)$$

Equation 2 $$d = a_o/(h^2+k^2+l^2)$$

where a_o is the lattice parameter and (h,k,l) are the Miller Indices of the reflecting planes (10).

SEM was conducted on a Hitachi S-2500 with an Oxford X-ray Energy Dispersion Spectrometer. An accelerating voltage of 20 KeV was used. Semi-quantitative analysis was used to estimate the chemistry. This voltage is sufficiently high to interrogate material to a depth of 50 nm so the chemical composition does not have high confidence. XRF was conducted on a Spectrum S Lab 2000 unit. A sample blank was tested in addition to the actual sample for comparison.

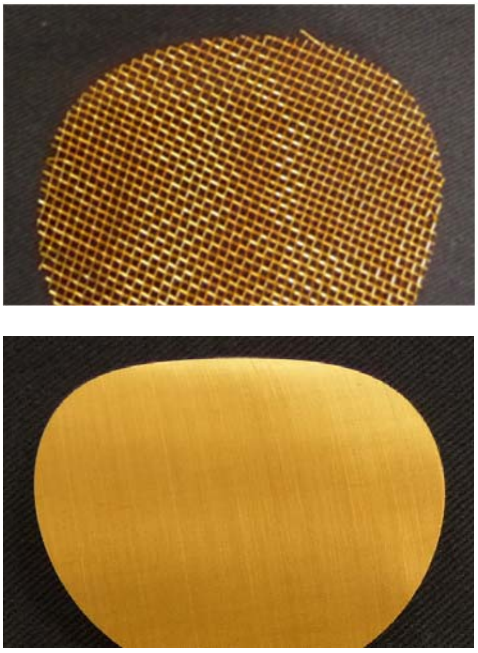

Figure 2. As received copper (upper) and bronze (lower) screen material.

Results and Discussion

Zinc capture tests for copper screens were conducted from 250°C to 550°C and from ambient to 550°C for bronze screens. The appearance of the as-received screens is shown in Figure 2. A fairly coarse mesh copper screen and a finer mesh bronze screen were used. These screens were selected to minimize adverse evacuation effects for the high vacuum system, although previous work indicated that filters with pores larger than 10 µm did not adversely affect pump-down times (3). The effectiveness of the screens for trapping zinc vapors can be inferred from the data in Table 2 and Table 3. These data show some deposition at low temperatures and losses at other temperatures. The mass losses for the copper screen are due primarily to wires being detached from the screen. Due to the coarseness of the screen and sample preparation, the wires at the edges were frequently inadvertently removed. A

loose wire filament on the top of the screen is shown in Figure 2. For some of the latter tests, the testing method was modified to reduce this tendency, but this modification was not completely successful in preventing wire loss.

Figure 3. Zinc Pot showing residual zinc charge, cleared area and zinc deposit on sidewalls.

Figure 3 shows the zinc pot after a typical experiment. The zinc pot exhibited a clean sidewall where the mantle heater exceeded about 325°C. The areas on the sidewall where the temperatures were less than 325°C resulted in a fairly thick zinc deposit. This result is consistent with the zinc vapor pressure diagram shown in Figure 4. Note that the nominal conditions for the heater mantle are indicated in Figure 4: the expected pressure of zinc is 1.4 x 10^{-5} ATM (0.011 Torr). A typical thermal / pressure profile for a vapor deposition at 350°C is shown in Figure 5. One can see that there are

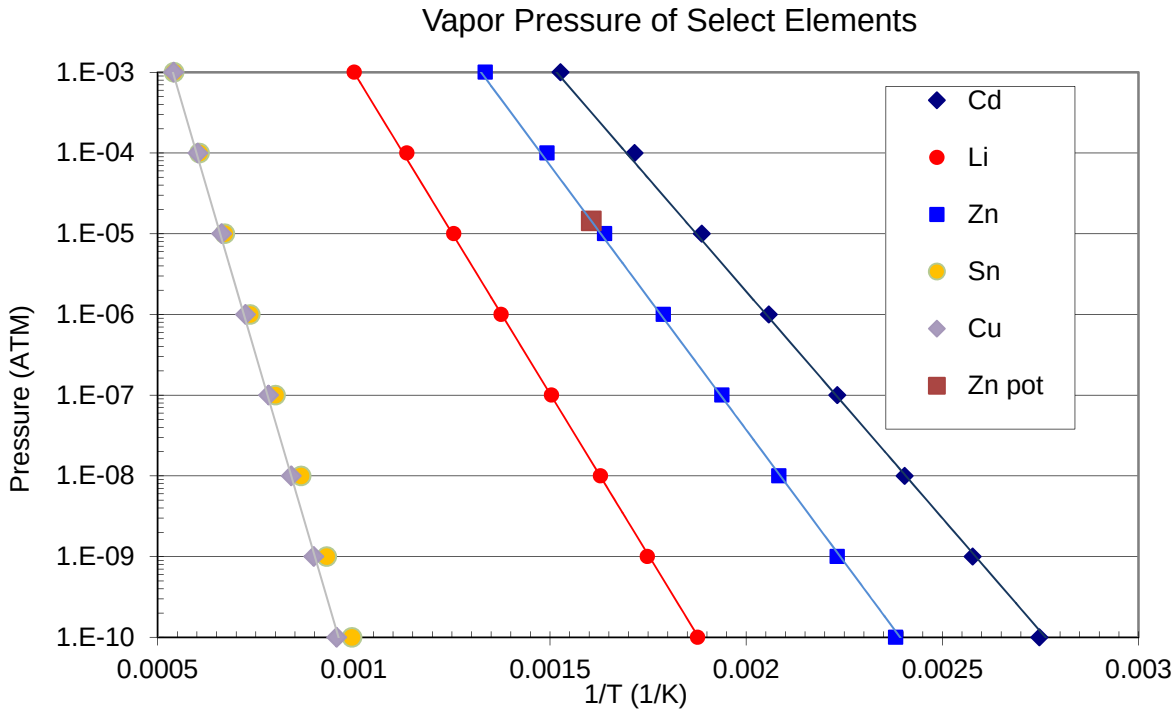

Figure 4. Vapor pressure of select elements and the test conditions.

two pressure spikes due to heating the filter and the zinc pot. These pressure increases are due to the off-gassing of the vessel walls in addition to the vaporization of the zinc. In order to characterize these pressure changes and to attribute them to off-gassing and vaporization increases, respectively, experiments were conducted with an empty zinc pot heated to 350°C with the filter at ambient conditions and with the filter at 350°C; these data are presented in Figure 6. The blue line is for the ambient filter region and the red line is for the 350°C filter, these data show and increase in pressure when heating just the zinc pot is about 100 times lower than the observed pressures for heating the filter area alone and the system pressure during a zinc vaporization test. From these experiments, it is surmised that the zinc vaporization rate can be accommodated by the vacuum pump and that the total pressure is less than the equilibrium zinc vapor pressure, Figure 4. This data shows that the system is able to remove any excess zinc vapor and cause it to deposit in the locations where it is preferred.

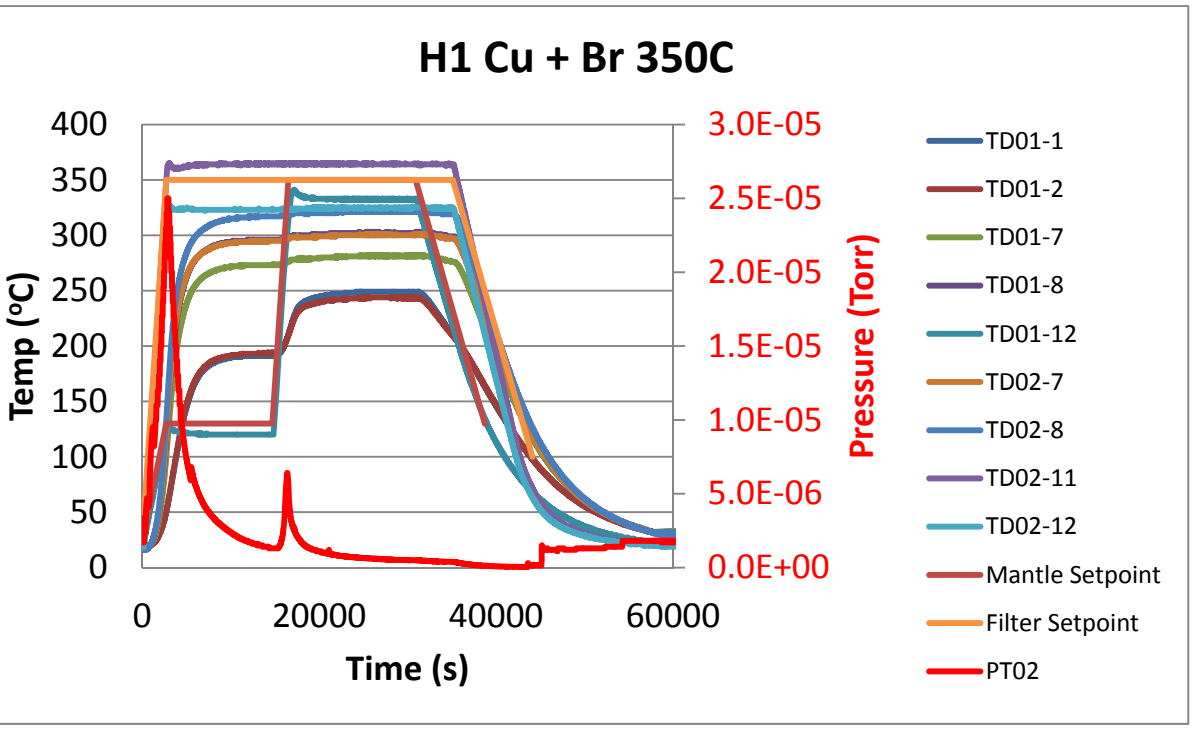

Figure 5. Thermal and pressure profiles for experiment H1 with the zinc pot and filter temperatures set at 350°C.

Figure 7 and Figure 8 show the appearance of copper and bronze screens, respectively, from low to high temperature filter exposures. The temperatures indicated are the filter set-points not the actual temperatures. At low temperatures, less than 250°C, there is a gray metallic zinc deposit present on the surface. As the set-point temperature increases; the screens undergo a coloration change from grayish deposits to golden to reddish copper color at higher temperatures. These changes are fairly subtle and difficult to observe in Figure 7 and Figure 8. The second 350°C sample is an exception since it clearly appears gold.

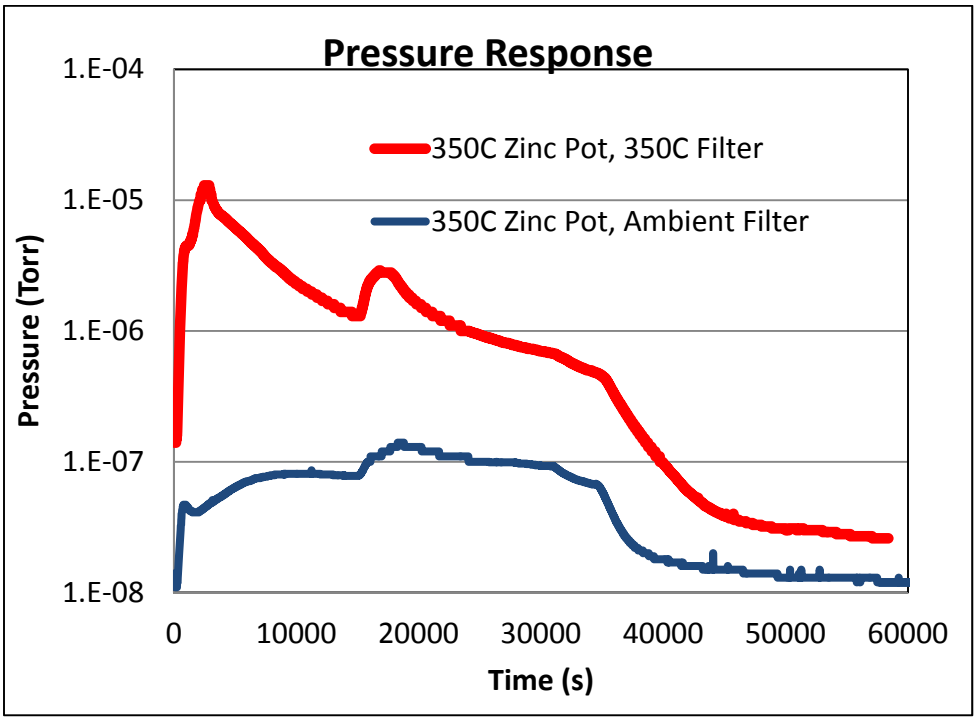

Figure 6. Pressure vs. time for baseline conditions for the filter at ambient and 350°C.

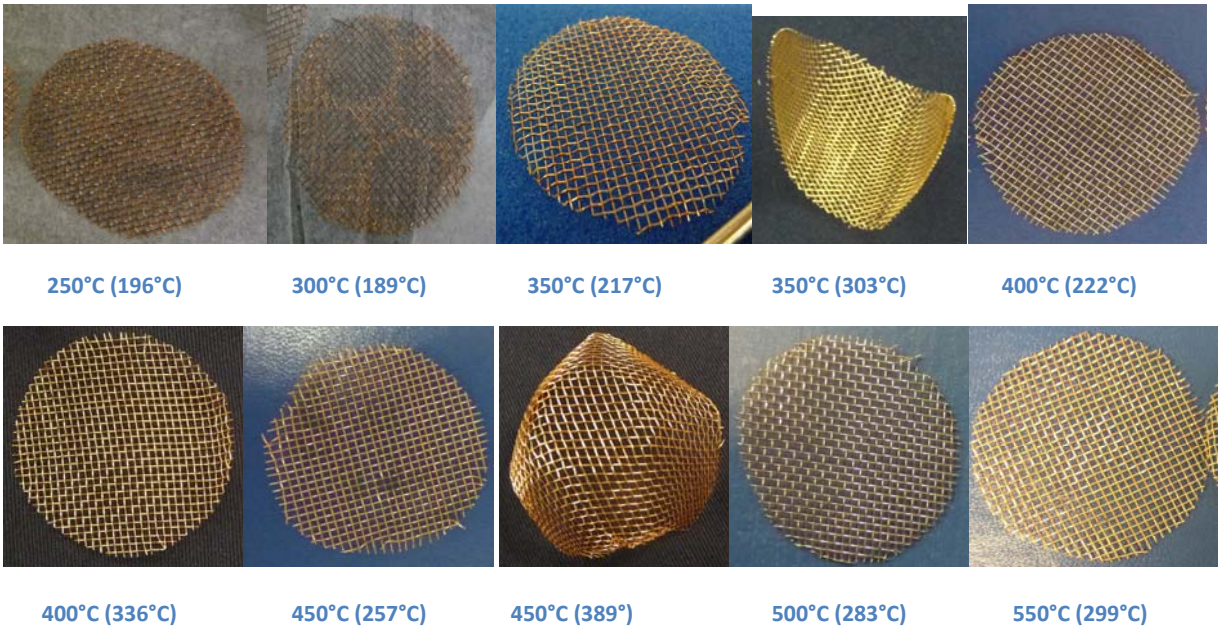

Figure 7. Photographs of copper screens after testing with the filter controller set between 250-550°C. Note the Zn on the 300°C sample and the golden color of the second 350°C sample, (measured temperatures from Table 2).

The weight change data from these experiments are shown in Figure 12 and presented in Table 2 and Table 3. There is not an obvious relationship between the weight gain and the filter set-point temperature; note that there are several inconsistencies in the test data with respect to the weight gains and color changes for the copper screens. In one case (450°C) there was minor weight gain while in the other it exhibited the highest gain. An examination of the actual temperature versus the set-point temperature suggests that the high deposit occurred at a lower actual temperature (Figure 12).

Similar to the Cu screen results, the bronze screen test data indicates that near ambient temperatures, there is a significant weight gain, also indicated by the gray deposits on the screens, Figure 8. The deposits at lower temperatures are the result of physically trapping the zinc vapors but not having it chemically react. The deposits formed at ambient conditions are neither tightly adherent nor chemically bound, this result is consistent with the previous study (4) that indicated that 200°C resulted in superior adherence compared to lower temperatures. Thus it appears that temperature is more important than substrate chemistry for physical trapping.

As a way to increase the surface area for zinc vapor deposition and to modify the deposition surfaces, bronze strips were inserted into the filter housing, Figure 1. These strips exhibited varied success in capturing and trapping the zinc vapors, as shown Figure 9. Mostly consistent with the screen data, a bright golden color is observed for the strips exposed at set-point temperatures between 350°C and 450°C. These temperatures correlate to measured deposition temperatures of 200-300°C. The weight

changes exhibit a peak at a 400°C set-point with a measured temperature of 230°C. The zinc deposit reacted with the bronze strip to form brass.

Table 2. Copper test conditions and response for a mantle temperature of 350°C. Cu-2* was used to determine if reaction was feasible with a copper screen located in the Zn pot set at 400°C for extended periods of time

Test ID	Filter SP (°C)	Filter Bottom Temp (°C)	Filter Top Temp (°C)	Ext. Temp (°C)	Δ Temp (°C)	Δ SP – T_{ave} (°C)	Screen 1 (mg)	Screen 2 (mg)	Screen 3 (mg)	Screen 4 (mg)
Cu-2*	NA	NA	NA	NA	NA	NA	NA	NA	NA	NA
Cu-6	250	196	197	282	32	-53.5	1	0.5	1.4	1.5
Cu-5	300	189	191	277	-23	-110	-2.2	-2.7	1.2	1.4
Cu-7	350	217	224	327	-23	-129.5	-2.7	2.2	1.6	1.4
Cu-16	350	303	282	323	-27	-57.5	1.4	1.5	0.8	
Cu-8	400	222	236	370	-30	-171	0.2	-0.1	0	0.3
Cu-12	400	336	306	375	-25	-79	-5.6	0.2	0.3	1
Cu-9	450	257	267	420	-30	-188	8	-7.4	0.1	10.3
Cu-15	450	389	354	425	-25	-78.5	0.2	-0.2	0.2	0.2
Cu-10	500	283	297	469	-31	-210	5.3	0.4	-0.1	-0.9
Cu-11	550	299	280	521	-29	-260.5	1.8	3.2	-2.7	5.1

The distinct color change from copper orange to bright brass suggests that zinc and copper have alloyed. The amount of alloying can be estimated by shifts in the lattice parameters. XRD is somewhat useful for this study since it interrogates only a few nm to µm of the surface material. To make the technique more useful for these experiments, a calibration curve was derived from the powder diffraction data files (PDF) and literature (9). The calibration curve for the increase in lattice parameter as a function of solute additions for copper with Sn and Zn is shown in Figure 10. Based on phase diagrams and other information, copper can accommodate up to 30% solute with linear increases of lattice parameter. Selected samples were evaluated with XRD including a copper screen sample that was placed in the zinc pot during vaporization. This sample exhibits the diffraction pattern shown in Figure 11. The peak doublets are due to the presence of an intermetallic compound of Cu_3Zn.

The XRD patterns from the other samples exhibited peak shifts due to alloying. The average lattice parameters were calculated using Equation 1 and Equation 2. The resultant lattice parameters are presented in Table 4. These data indicate that the copper screen may have incorporated up to 22% Zn near the surface while the bronze may have incorporated up to 15%. Neither composition is well known due to the error involved in these measurements. In addition, the bronze alloying estimates are complicated by the lattice parameter shift caused by the 5% tin alloying. Regardless of these contributions to the measurement error, these data still show that alloying has occurred to a certain extent.

Table 3. Bronze test conditions and responses for a mantle temperature of 350°C.

Test ID	Filter SP (°C)	Bottom Temp (°C)	Top Temp (°C)	Ext Temp (°C)	Δ Temp (°C)	Δ SP - Tave (°C)	Screen 1 (mg)	Screen 2 (mg)	Screen 3 (mg)	Screen 4 (mg)	Strips (mg)
Br-6	500	75	64	35	-465	-430.5	0	0.9	4.1	0.3	0.3
Br-8	550	87	75	45	-505	-469	0.3	1.7	6.6	0.4	0.4
Br-1	250	130	126	235	-15	-122	0.5	1.4	3.5	0	
Br-2	300	209	190	315	15	-100.5	0.9	0.5	0.9	0	0.5
Br-3	350	217	200	348	-2	-141.5	0.3	0	0.4	0.3	1.2
H-2	350	283	258	346	-4	-79.5	0.1	0.3	0.2	0.4	1
Br-4	400	293	317	394	-6	-95	0.1	0.1	0.2	0.3	1.5
Br-5	450	311	335	445	-5	-127	0.9	0.3	0	0	0.8
Br-7	500	353	390	486	-14	-128.5	0.3	0.1	0.1	-1.4	0.2
Br-9	550	435	470	518	-32	-97.5	0.4	0.6	0.4	0.6	0

To better elucidate the composition, samples were examined with XRF. A strip of bronze exposed in experiment H-2 (Table 3) was tested and it had 1.95% Zn at the end nearest the Zn source and 0.43% Zn at the other end. The strip exhibited a uniform gold color despite the measured range of zinc content. In addition, a piece of copper screen was measured and it indicated approximately 0.4% Zn. The measurement of the screen presented challenges since it is not a solid surface and much of the signal may be lost.

Table 4. Lattice parameters determined from the XRD of the samples. The sample IDs are correlated to Table 2 and Table 3. BL refers to baseline.

Sample ID	Lattice Parameter	Alloy Content
Cu Screen BL	0.3606	-2.2
Cu-2 Screen	0.3666	22.3
Cu-2 Screen	0.3605	-2.3
Br Screen BL	0.3670	9.6
Br Plate BL	0.3651	6.2
Br-4 Screen	0.3665	15.0
Br-4 Plate	0.3643	5.9
Br-1 Screen	0.3633	2.8

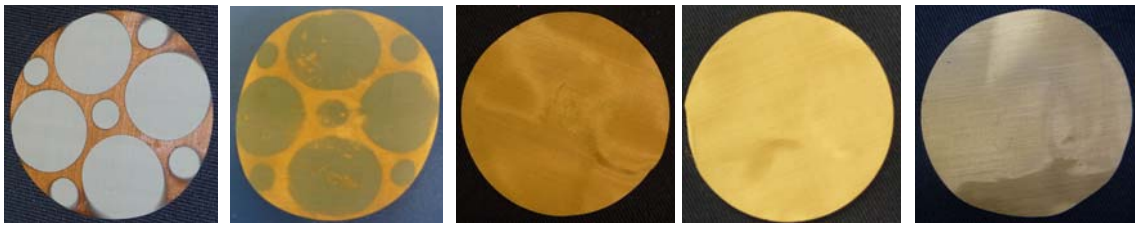

Ambient (75°C) 250°C (130°C) 300°C (209°C) 350°C (217°C) 350°C (283°C)

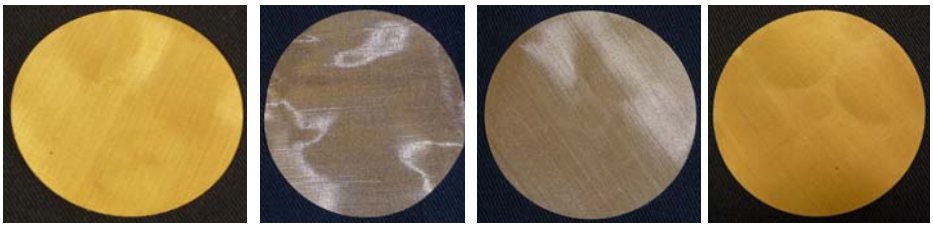

400°C (293°C) 450°C (311°C) 500°C (353°C) 550°C (435°C)

Figure 8. Appearance of bronze screens after exposure to Zn vapors with the set point and (measured) temperatures indicated (Ref.Table 3).

Ambient (75°C) 250°C (130°C) 300°C (209°C) 350°C (217°C) 350°C (283°C)

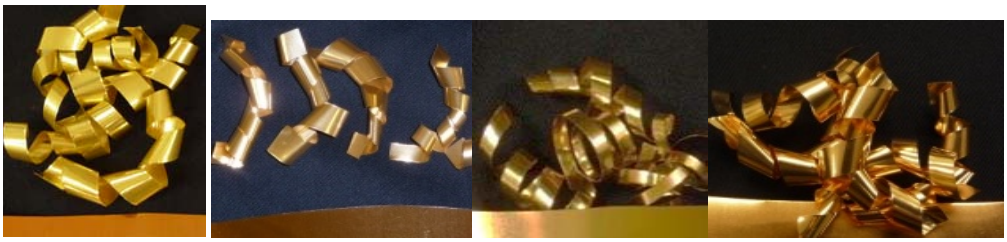

400°C (293°C) 450°C (311°C) 500°C (353°C) 550°C (435°C)

Figure 9. Appearance of bronze strips after exposure to Zn vapors with the set point and (measured) temperatures indicated (Ref. Table 3).

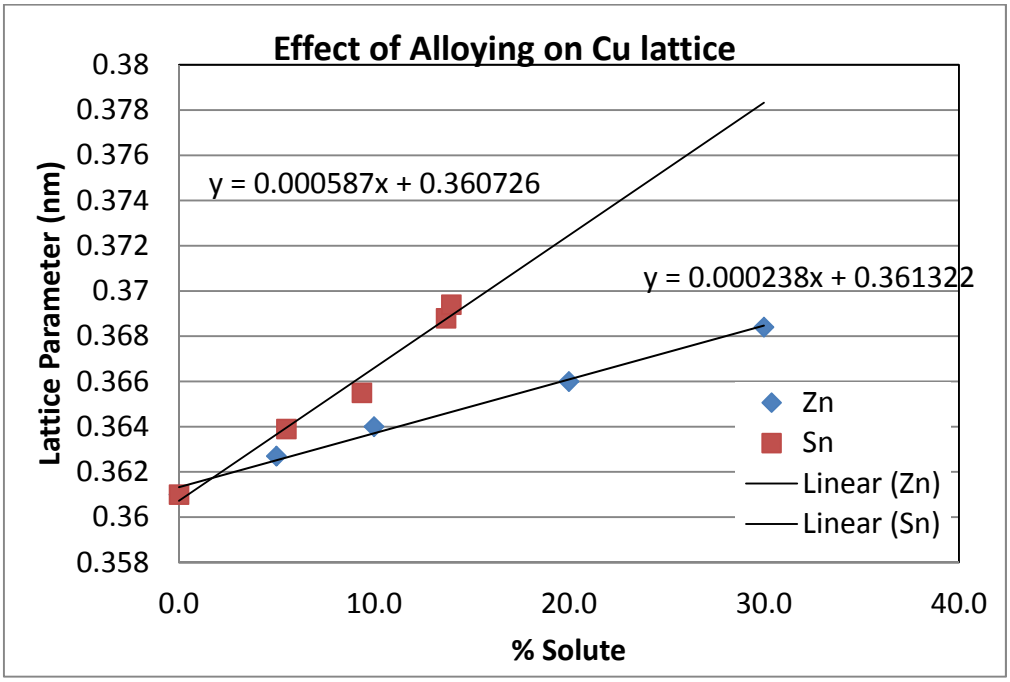

Figure 10. Effect of alloying on lattice parameter for copper alloyed with Sn and Zn.

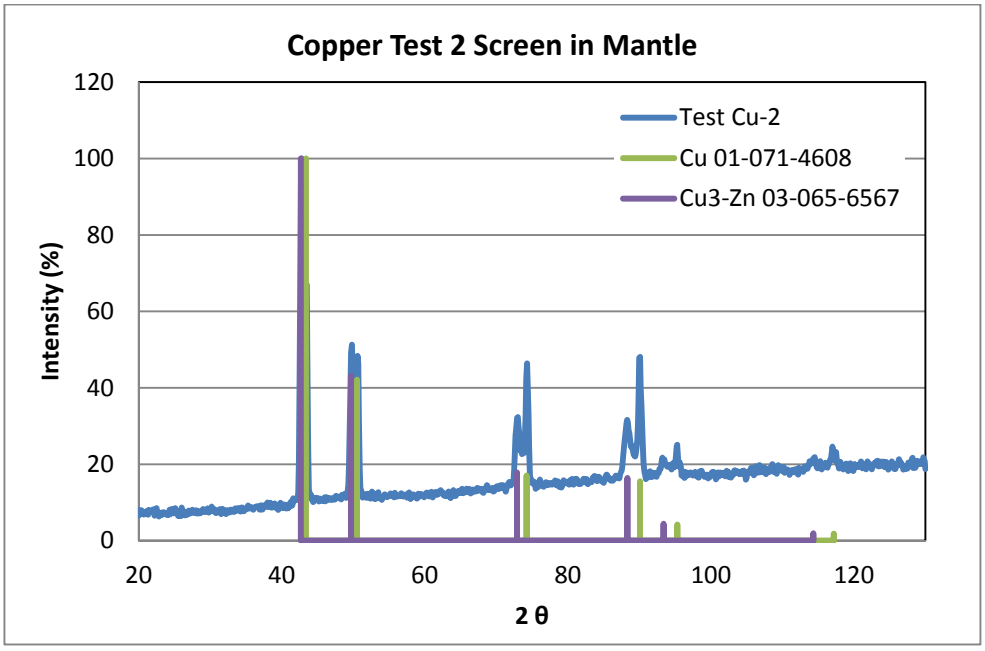

Figure 11. XRD scan from a copper screen that was placed in the mantle for Test Cu-2 and that indicates the presence of Cu and Cu_3Zn.

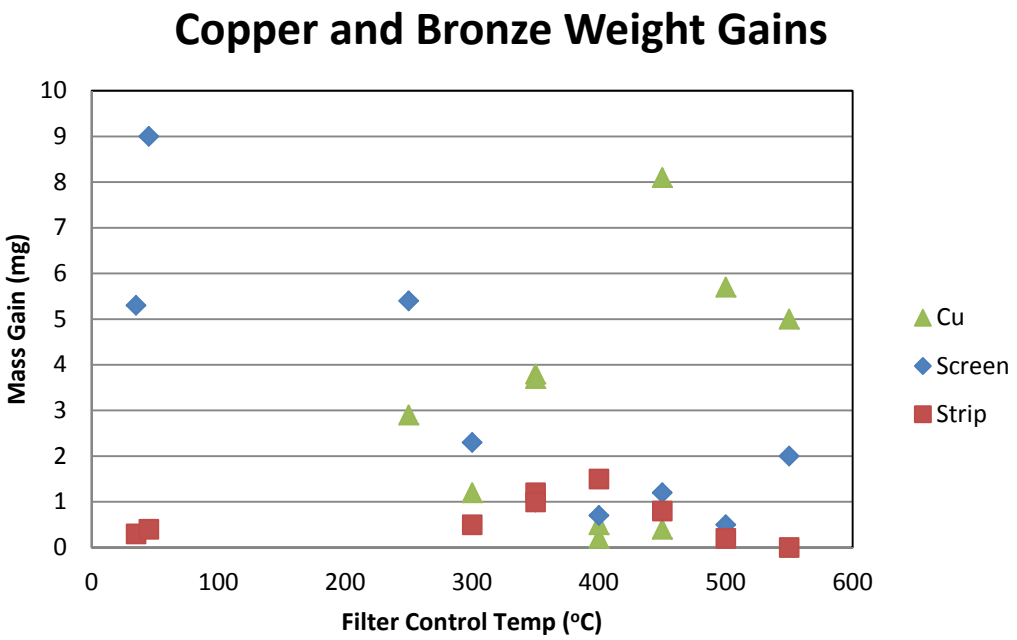

(a)

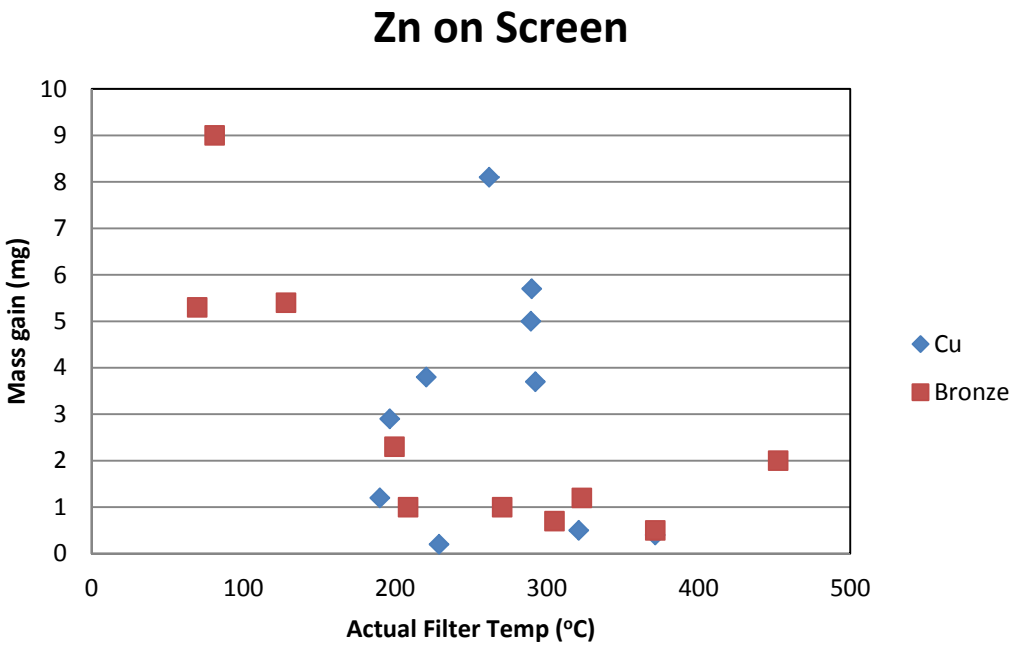

(b)

Figure 12. Mass gain for copper and bronze screen s with the filter control temperature between 250 and 500°C and the mass change as a function of the actual filter temperature.

Scanning electron microscopy was used to examine the deposit morphology and the near surface chemistry. The surface morphology of the bronze screens is shown in Figure 13, Figure 14, and Figure 15. It is interesting to note that the number and size of the zinc rich deposits vary with deposition temperature. For the samples that were examined, there are fewer but larger deposits at 350°C than at either 400°C or 450°C. There seems to be a maximum at 400°C for the number of deposits; this maximum in deposit number also corresponds to a maximum in weight gain. The actual temperature for deposit ranged between 293°C and 317°C based on thermocouples seven and eight, Table 3.

The bulk composition of the light and dark area, denoted 1 and 2, respectively, was determined using X-ray Energy Dispersion Spectroscopy (XEDA). The light and dark areas were consistently produced Cu, Sn, and Zn and Cu and Sn, respectively. The composition of the deposits was determined using the semi-quantitative analysis program with the results indicated in Table 5. Note that the dark areas are generally Zn free and that there may be a significant Zn contribution to the signal. These results are semi-quantitative since the algorithm uses many simplifications and the beam may have been placed such that it interrogated the strip material in addition to the Zn deposit or it may have penetrated the Zn deposit. None-the-less, the large Zn particles from the Br-3 experiment (350°C) were sufficiently large to completely involve the electron beam. The deposits on Br-4 and Br-5 may not have been.

Table 5. Semi-quantitative analysis (weight %) of bronze strips from experiments Br-3, Br-4, and Br-5.

	Sample/ Location	% Cu	% Zn	% Sn
Br-3	350°C/Light (1)	59.1	39.4	0
Br-3	350°C/Dark (2)	95.3	0	4.7
Br-4	400°C/Light (1)	88.8	7.0	4.3
Br-4	400°C/Dark (2)	93.7	1.6	4.7
Br-5	450°C/Light (1)	90.7	6.1	3.1
Br-5	450°C/Dark (2)	95.4	0	4.6

A cross section of the bronze strip material was mounted in epoxy and examined visually and in the SEM. The optical and electron micrographs are shown in Figure 16. There is no visual evidence of a reaction layer, however, semi-quantitative XEDA was conducted with the results shown in

Table 6. It is apparent that there is interdiffusion between the substrate and the zinc deposit and that the zinc is not solely present on the asperities shown in surface SEM images of Figure 13, Figure 14, and Figure 15.

Table 6. Semi-quantitative results from the areas shown in Figure 16. Contaminants are from mounting material.

Location	w/o Cu	w/o Zn	w/o Sn	Other (contaminants)
1	88.5	2.9	4.4	2.0 O,0.8 Al, 1 Si, 0.5P
2	90.1	1.8	5.2	1.4 O, 0.7 Al, 0.6 Si, 0.4 P
3	94.0	-	4.9	0.6 O, 0.5 P
4	75.3	4.5	4.8	3.2 O, 5.2 Al, 7 Si
5	93.2	-	4.9	0.9 O, 0.3 Si, 0.6 P

Summary and Conclusions

Zn will react with both copper and bronze screens to produce brass. In addition, bronze strips will react to form brass. There is a relatively small temperature range between 200°C and 335°C in which zinc vapors are captured and converted via a diffusion mechanism to brass. At lower temperatures the zinc remains a non-reacted loosely adherent deposit while at higher temperatures it tends to remain a vapor and not deposit.

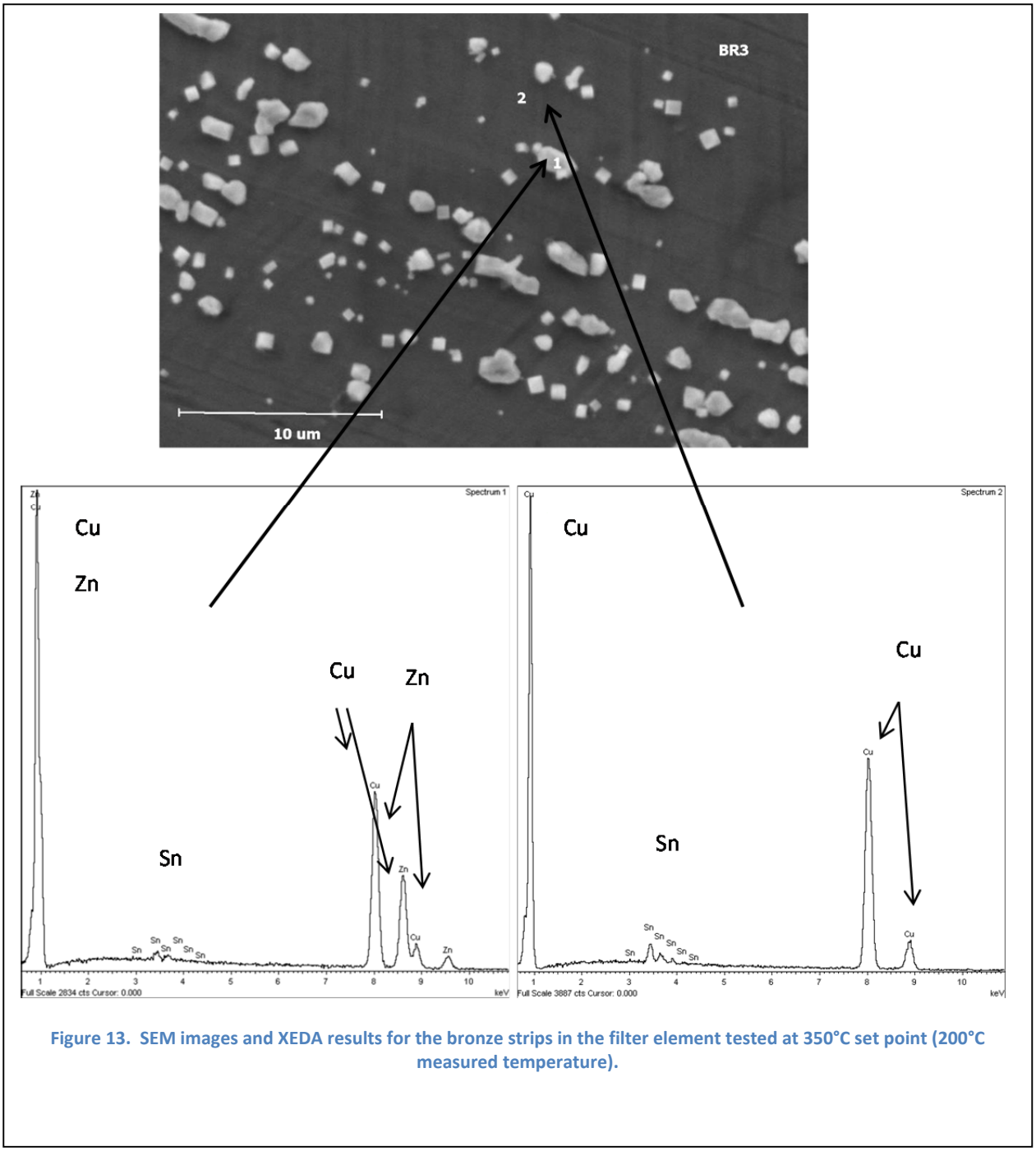

Figure 13. SEM images and XEDA results for the bronze strips in the filter element tested at 350°C set point (200°C measured temperature).

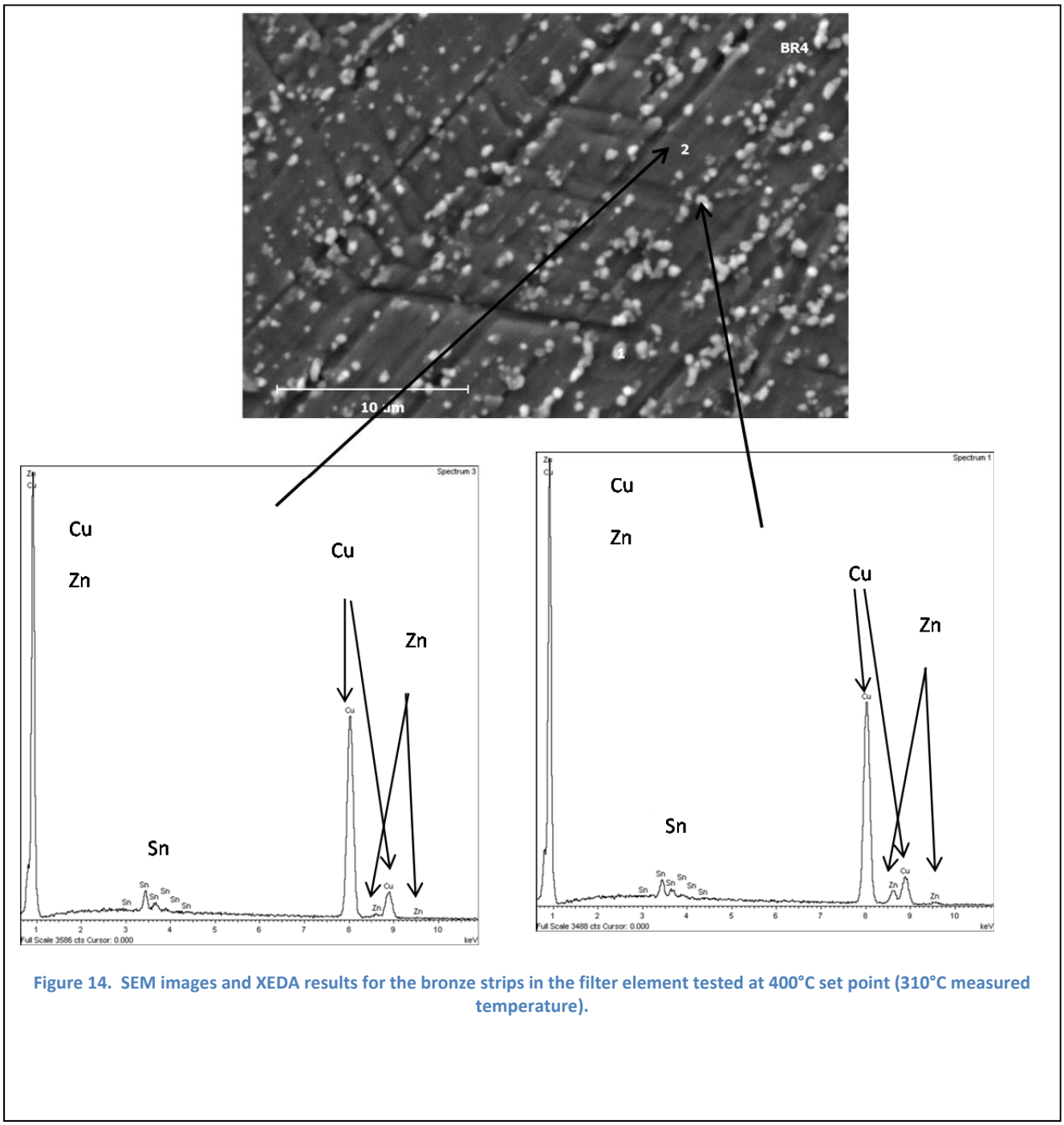

Figure 14. SEM images and XEDA results for the bronze strips in the filter element tested at 400°C set point (310°C measured temperature).

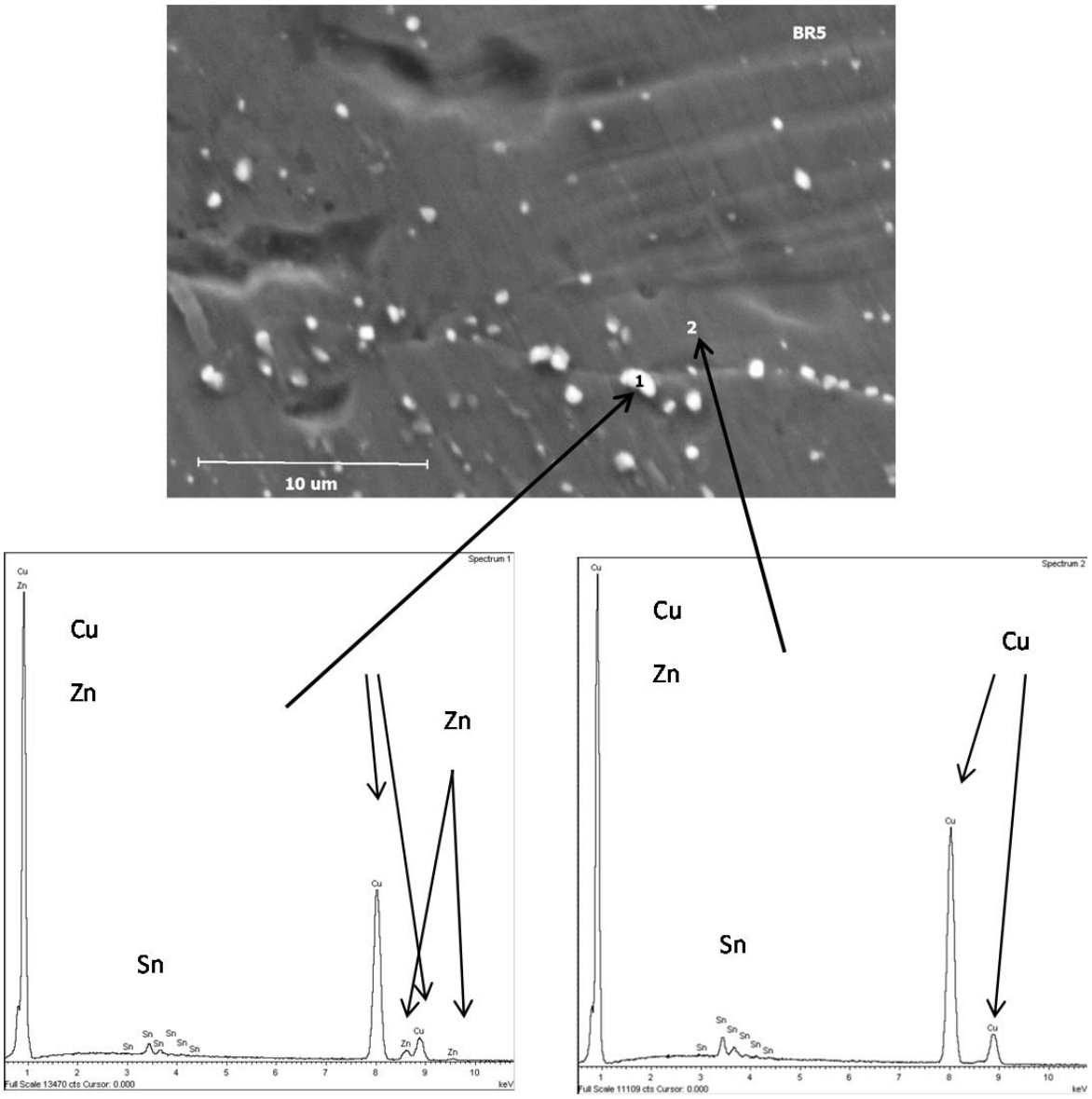

Figure 15. SEM images and XEDA results for the bronze strips in the filter element tested at 450°C set point (320°C measured temperature).

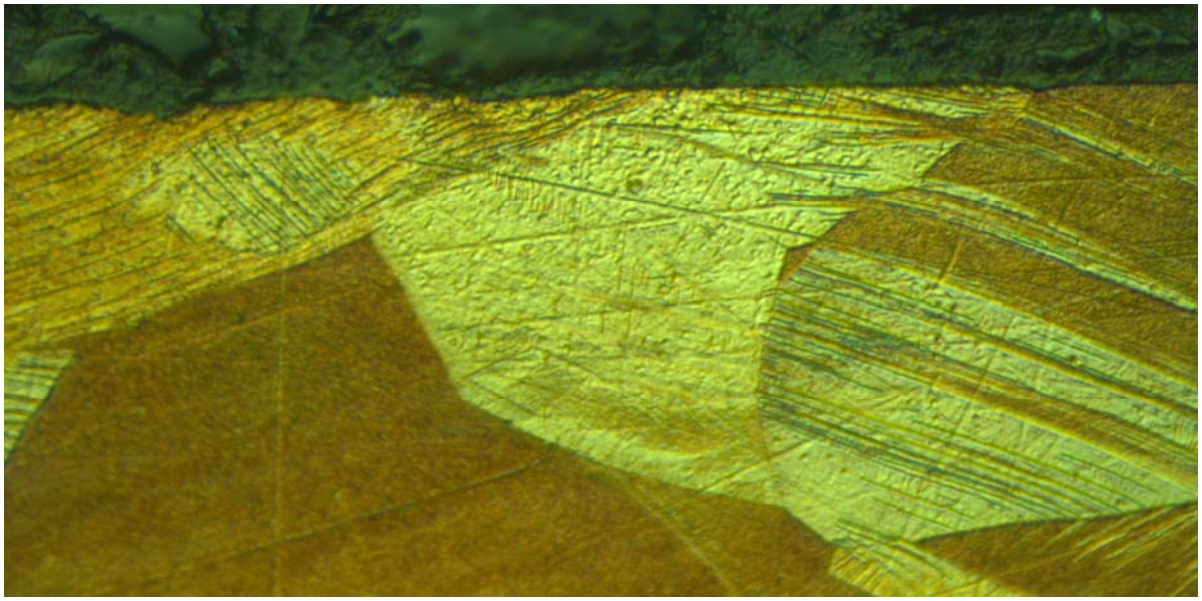

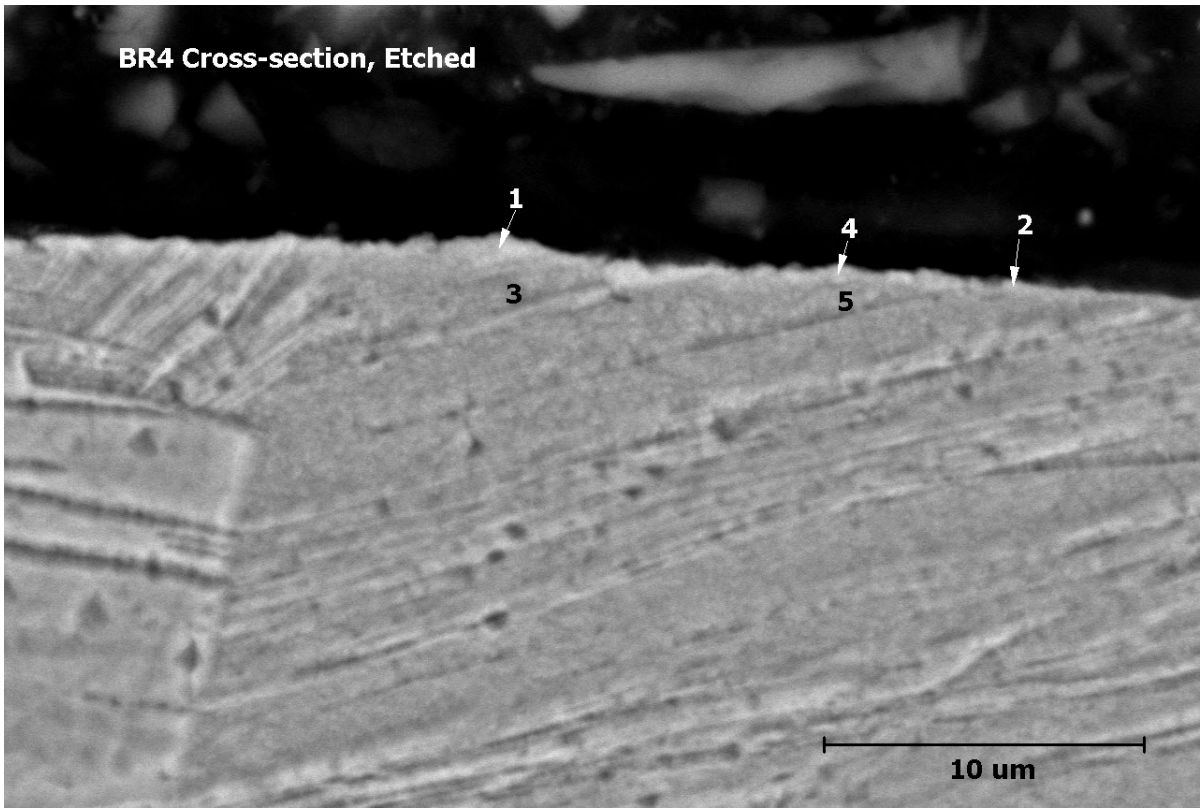

Figure 16. Optical and Scanning electron micrographs of sample Br-4 (400°C Control 300°C actual) strip.

Recommendations

Additional testing is needed to (1) determine if other bronze alloys will exhibit enhanced brass formation at lower temperatures (2) determine if simple surface treatments can enhance the deposit efficiency (3) determine if the brass is stable in the deposition conditions and (4) determine if the extraction gas composition will have an adverse effect on the surfaces and preclude deposition of zinc.

Acknowledgments

The author would like to recognize the contribution of Craig Stripling for assembling the apparatus and the contributions of Katelyn Kessinger and Jonathan Baker, summer interns from Colorado School of Mines and Clemson University, respectively, for conducting experiments and performing sample analysis. He would also like to acknowledge the efforts of Mary Anton and Tony Curtis for their help with SEM analysis. He would like to thank Adrian Mendez-Torres for his assistance with XRD analysis. He also appreciates the technical support of Kevin Stoner and the programmatic support of Bob Snyder. This work was conducted in support of DOE contract DE-AC09-08SR22470.

References

1. SRNL-L7100-2009-00013, Recommendations for TEF to Minimize Further Contamination of ^{65}Zn, P. Korinko, A. J. Duncan, R. A., Malstrom, May 2009
2. SRNL-STI-2010-00473, Zinc Mitigation Interim Report – Thermodynamic Study, P.S. Korinko, Dec 17, 2010
3. SRNL-STI-2011-00347, Effect of Pore Size on Trapping Zinc Vapors, Paul Korinko, December 17, 2010
4. SRNL-STI-2011-00348, Effect of Filter Temperature on Trapping Zinc Vapor, Paul Korinko, March 25, 2011
5. SRNL-STI-2011-00349, Preliminary Study of Methods to Chemically Bind Zinc, Paul Korinko, June 10, 2011
6. SRNL-TR-2011-00350, Summary Report for Zinc 65 Contamination Control, Paul Korinko
7. SRNL-L4410-2012-00006, Zinc Deposition R&D Directions, P. Korinko, Sept 2012.
8. PDF Card No.: 01-071-4608, Copper
9. Properties and Selection: Nonferrous Alloys and Pure Metals, ASM Metals Handbook, Volume 2, 9th Edition, ASM International, Metals Park, Ohio, pp.316-330, (1986).
10. Elements Of X-Ray Diffraction, D.B. Cullity, Addison-Wesley Publishing Company, Inc. Reading, MA, 1956.